EFFECT OF PRIOR MICROSTRUCTURE ON AUSTENITE DECOMPOSITION AND ASSOCIATED DISTORTION

REPORT

AUGUST 2001

R. Ramanathan and R. P. Foley

MMAE Department
Illinois Institute of Technology
10 West 32nd Street
Chicago, IL 60616-3793

312-567-3052p / 312-567-8875f / foley@iit.edu
http://mmae.iit.edu/~foleyweb/
http://mmae.iit.edu/~tpc/

INTRODUCTION

Steel components are heat treated in order to obtain desired microstructure and properties. However, such heat treatments often also impart unwanted and often unpredictable dimensional changes [1]. In the present work, Jominy bars are used to characterize the pattern of the dimension change versus distance from the quenched end and versus initial starting microstructure. The behavior of nine different kinds of steels is investigated.

Size distortion is characterized as part growth or shrinkage. It is generally attributed to the volume differences between the various phases developed in the microstructure of a steel component during heat treatment. The martensitic microstructure of a particular steel, for example, has a slightly higher specific volume (lower density) than the same steel with a ferrite-pearlite microstructure. The specific volume differences between the various phases generally increase with the alloy carbon content. Shape distortion is associated with mechanisms that produce microstructure variations within the component. These microstructure differences may be inherited from casting and hot working or may result from an uneven thermal cycle.

Experiments with carburized and oil-quenched annular discs produced from different steels have shown that the dimension changes could be related to steel hardenability. The dimensional changes were found to be a function of steel hardenability only as long as the alloy composition was insufficient to through harden the part so to produce a 100% martensitic core. Disks made from alloy compositions with sufficient hardenability all showed similar distortion behavior [1]. In general a majority of the variability in distortion behavior can be related to the variability in the transformation behavior of the steel used to make the part and the variability in the thermal cycle used to process the part. Sensitivity to distortion variability seems to be related to the consistency with which a particular steels austenite decomposes to produce a specific microstructure distribution within a part.

Factor influencing the austenite decomposition include the alloy chemistry, the austenite grain size, and the local cooling path. As a result, similar cooling paths lead to similar distortion patterns and the decomposition of austenite in similar fashion leads to similar distortion pattern. Fukuzumi and Yoshimura showed that small variations in aluminum content (Al/N ratio) in 8620 and 4120 low-alloy steel produces pronounced distortion pattern differences in Navy C-rings that may be related to differences in the CCT (continuous cooling transformation) behavior of the steels [2].

Microsegregation in large-tonnage low-cost steel products is unavoidable. Alloy solidification behavior during casting and the subsequent hot working process produces elemental banding and possibly microstructure banding as well. Elemental banding results from interdendritic segregation and is related to the difference between the alloy liquidus and solidus temperatures. Microstructure banding results from carbon diffusion to regions of the microstructure where elemental banding produces a high local affinity for carbon and the subsequent decomposition of these regions into various austenite decomposition products. Microstructure variability associated with microsegregation of alloying elements has been postulated as being one of the likely important contributors to hardness and geometry variations of forged and heat-treated

components [3]. Such segregation produces a position sensitive alloy composition and transformation behavior. These effects may lead to complicated distortion and residual stress patterns. In high-carbide tool steels, for example, size change directionality due to heat treatment has been attributed to microstructure changes associate with the redistribution of carbides from a state of preferential alignment to one of more random alignment [4].

Transformation of austenite is routinely characterized by the Jominy end-quench test. In this work, the end-quench test is used to characterize the transformation and distortion behavior of nine different types of steels. Hardness profiles, the common result of such test, are combined with measurements of diameter change to characterize the relationship between alloy chemistry and prior microstructure on the hardenability and distortion pattern developed in the steels.

Figure 1 shows a conventional flat machined in the Jominy by removing 0.015in layer along its length. A diameter variation along the length can be seen as an hourglass shape on a close look at the ground strip, the difference in the diameter of the bar at various distances from the quenched end results from the decomposition of austenite [3].
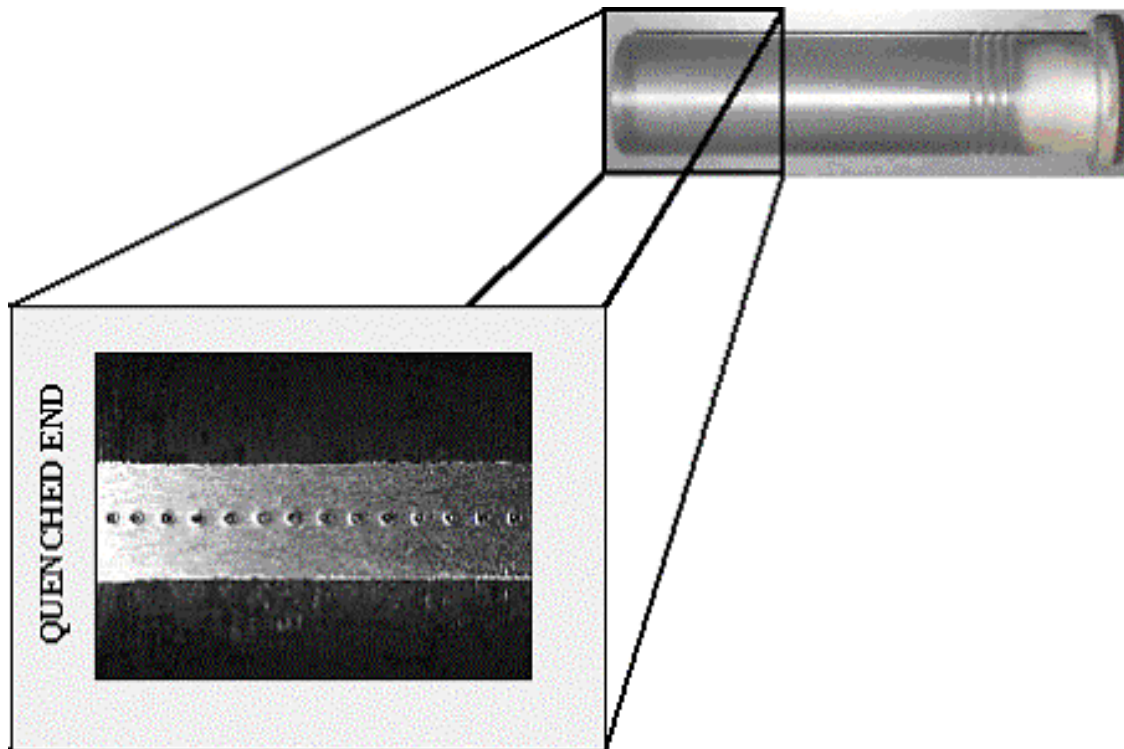

Figure 1 – Hourglass distortion patterns can be seen near the quenched end in flat ground in the Jominy bars due to diameter variation along the length.

3

EXPERIMENTAL PROCEDURE

Table 1 shows the chemical compositions of the nine steels used in this investigation. Some of the steels were selected such that they fairly represent the steels used in the forging industry and the others were selected because they may offer insight to the mechanism responsible for the distortion pattern. The steel set consisted of machinable grade 12L14 and 1117, plain low carbon 1018 steel, carburizing grade 8620 alloy steel, low hardenable, medium carbon 1045 steel, high hardenable, medium carbon 4140 steel, W1 and O1 tool steel and 304 austenitic stainless steel. The steels were purchased as bar stocks of 1.5in diameter. The chemical compositions of the steels were taken from literature.

TABLE 1 - Composition range of steel used in the present investigation (wt-pct).

Steel	C	Mn	Si	Ni	Cr	Mo	P	S	ELSE
1018	0.15-0.20	0.60-0.90					0.040 Max	0.050 Max	
1045	0.42-0.51	0.50-1.00	0.15-0.35				0.040 Max	0.050 Max	
1117	0.14-0.20	1.00-1.30					0.040 Max	0.08-0.13	
12L14	0.15Max	0.85-1.15					0.04-0.09	0.26-0.35	Pb 0.15-0.35
4140	0.38-0.43	0.75-1.00	0.15-0.35	0.25 Max	0.8-1.10	0.15-0.25			Cu 0.35 Max
8620	0.18-0.23	0.70-0.90	0.15-0.35	0.40-0.70	0.40-0.60	0.15-0.25	0.025 Max	0.025 Max	Cu 0.35
O-1	0.94	1.2	0.3		0.5				W 0.5
W-1	1	010-0.40	0.10-0.40	0.30 Max			0.025 Max	0.025 Max	W 0.15 Max
304 SS	0.08Max	2.00Max	1.00Max	8.0-10.5	18.0-20.0		0.045 Max	0.030 Max	

Figure 2 schematically shows the experimental procedures used in this work. Three 7in long sections were cut from the bar stock of the nine different steels and each of these three sections was individually heated to austenitizing temperature (900 +/- 5°C is maintained for all the bars) and held at this temperature for an hour in a laboratory box furnace. Following this, the bars were cooled in still air (air-cooled), in the furnace (furnace-cooled) or in oil (oil-quenched) to produce three different starting microstructures. Twenty-seven Jominy bars were obtained from nine different steels and three different initial microstructures thus produced. Jominy bars were machined in a HAAS SL – 20 CNC lathe. The sections from the end piece of the heat-treated bars were used to obtain metallographic samples for characterizing the initial microstructure in the longitudinal direction and the hardness profile across the diametric cross section.

The exact geometry of the Jominy bars were slightly different from the standard Jominy bars geometry in that each had a flat-machined perpendicular to the axis in the head and four grooves of specific dimension from specific distance from the end along the circumference of the Jominy bar. The purpose of the flat was to ensure similar positioning of the Jominy bars in the fixture
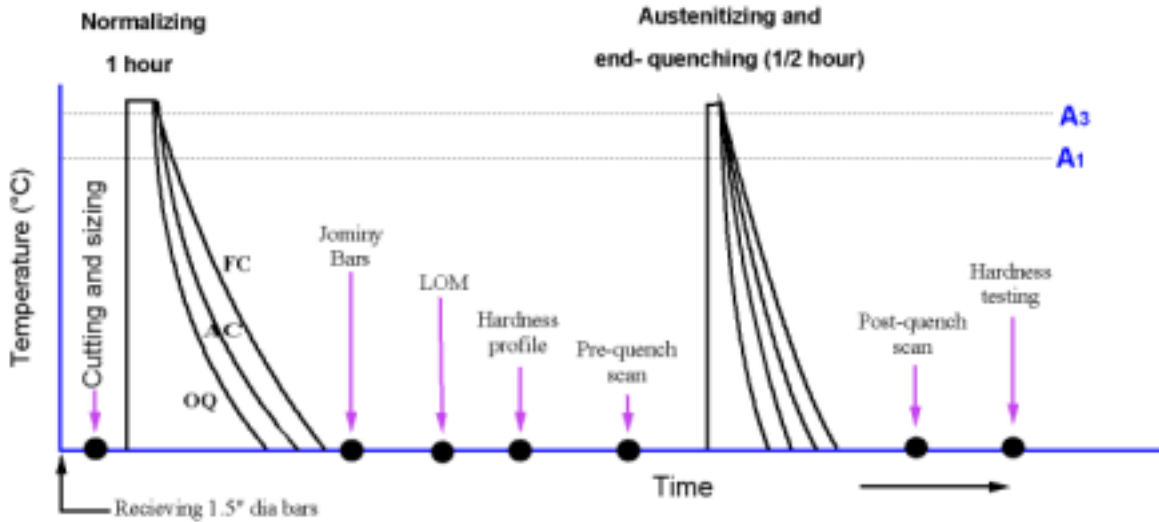
Figure 2 – Schematic overview of experimental test procedure

during the distortion measurements and the purpose of the grooves were to align the distortion data points before and after end quenching.

Distortion of the bars was characterized as change in bar diameter versus distance from quenched end. The diameter change was determined as the difference between the profile diameters measured before and after end quenching. The scanning of the Jominy bar was carried out in a Mitutoyo CBH-400 Contracer, this tracer was able to record vertical distance to 0.000008in and horizontal distance to 0.00001in. The Jominy bar was clamped in a jaw attached to an indexing head after ensuring that the flat in the jominy bar is parallel to the surface table using a dial gage with 0.0005in least count. The scanning was carried out along the length of the bar for every 30deg. The bar was then end quenched in confirmation with ASTM standard 255 [5]. The bars were heated to austenitizing temperature for 45min (900 +/- 5°C maintained for all bars) in a laboratory box furnace in a close fitting, closed-end stainless steel sleeve with cast iron pieces at the closed end to prevent oxidation. Since the head of the bar was not protected from oxidation by covering with a fixture the scale formed in the head was removed by a very mild sand blasting. The end-quenched bar was then scanned again in the Mitutoyo CBH-400 Contracer following the same procedure as before. The hardness measurement was also carried in confirmation with the ASTM standard 255 with flats ground to 0.015in and the hardness reported as the average of the hardness value from both the flats [5].

5

RESULTS AND DISCUSSION

Microstructures:

Figures 3 to 11 show the light optical micrographs of various steels along longitudinal direction of the bar under various heat treatment conditions. The microstructure of each steels in 100X and 400X original magnification are shown adjacently with furnace cooled (FC) on top, air cooled (AC) in the middle and oil quenched (OQ) at the bottom of the page for each steels.

In general, the microstructure refines as the cooling rate progresses from furnace-cooled to air-cooled to oil-quenched. The microstructure shows darker pearlite regions lighter ferrite regions and elongated inclusions are consistently seen with major axis in the longitudinal direction.

Banded ferrite-pearlite microstructures are noticed in the 12L14, 1117, 1018, 8620, 1045 and 4140 steels with banding wavelengths such that air-cooled samples have a smaller distance between neighboring bands of pearlite than furnace cooled samples. The microsegregation of manganese during solidification results in the banded microstructure of ferrite and pearlite that are observed in plain carbon steels [6]. Since manganese is austenite stabilizer manganese reduces the activity of carbon in austenite, the segregation of manganese also produces partitioning of carbon so carbon segregates with manganese [6]. The edges of pearlite bands are smooth in furnace-cooled condition and jagged in air-cooled condition. The banding effect in the longitudinal direction can be clearly seen in the lower magnification micrographs.

Banding is pronounced in steels containing ferrite and pearlite in about equal proportions [6], so we notice the banding effect is not pronounced in the O1 and W1 tool steels with higher carbon contents. The oil-quenched bars showed microstructure with virtually no sign of banding. The 4140 steel bars that are highly hardenable show martensitic microstructure even in air-cooled stage.

The 304-SS shows almost the same microstructure under all heat treatment conditions. The matrix of this austenitic stainless steel does not undergo phase transformation.

Figure 12 shows the hardness profile across the cross-section of the 1.5in bars, from which the Jominy bars are machined, after heating to austenitizing temperature and oil-quenching, air-cooling, furnace-cooling.

The hardness profile across the 1.5in bars uniformly show hardness decrease towards the center, which is due to the decrease in the cooling rate towards the center. The steels that have high hardenability like O1 and 4140 show large hardness variation between the oil-quenched, air-cooled and furnace-cooled condition, while less hardenable steels show lower hardness variations. Hardenable steels also show a low dip in hardness towards the center while low hardenable steels show a large dip in the profile. The 304-SS shows nearly the same hardness profile for all quenching conditions. The O1 steel shows the maximum hardness and the 12L14, 1117 steel that are machinable grade steels shows low hardness value.

12L14

12L14 FC — 200 μm

12L14 FC — 50 μm

12L14 AC — 200 μm

12L14 AC — 50 μm
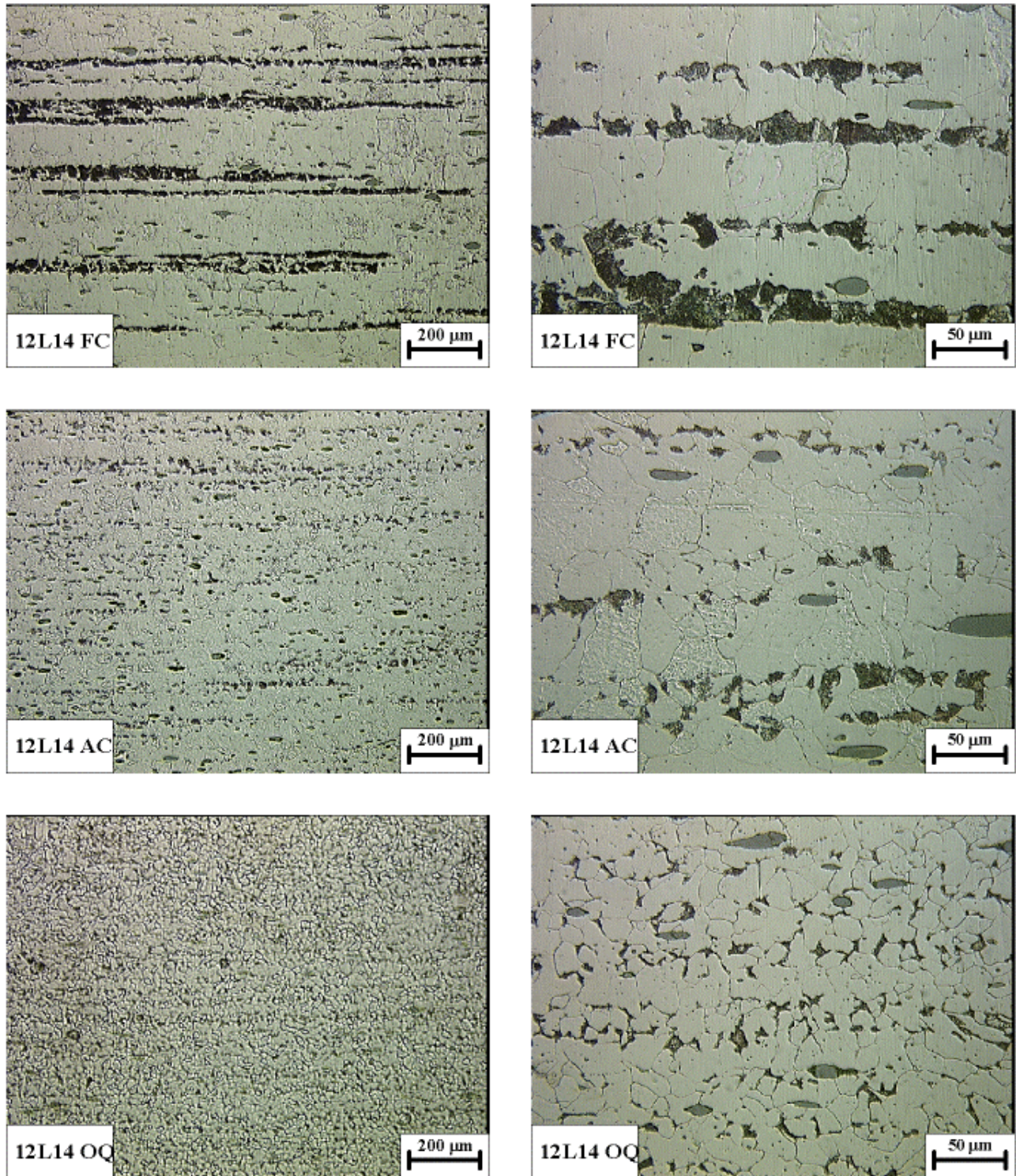
12L14 OQ — 200 μm

12L14 OQ — 50 μm

Figure 3 – Microstructure of 12L14 steel. Light optical micrographs, longitudinal sections, 2% nital etch.
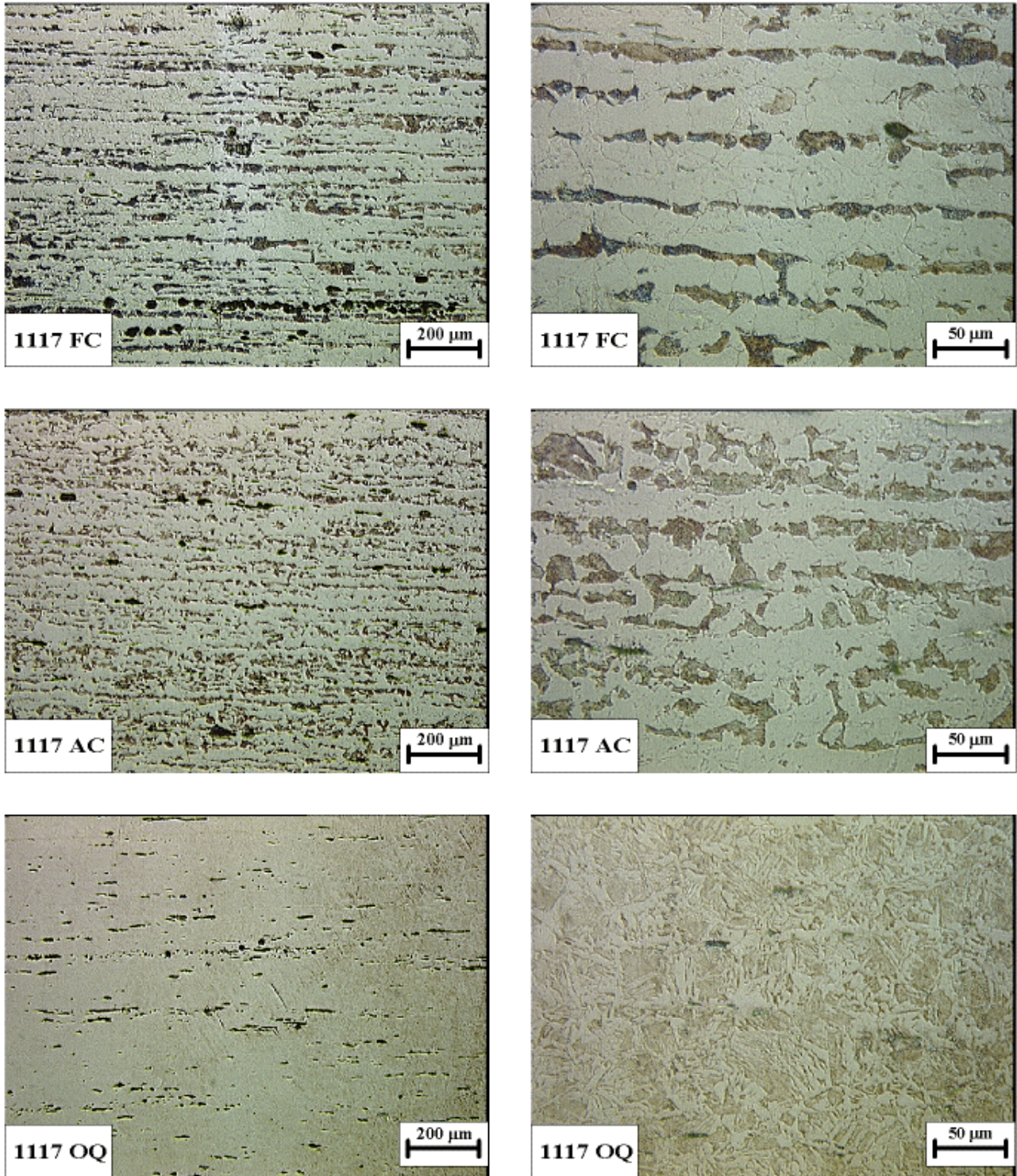
1117

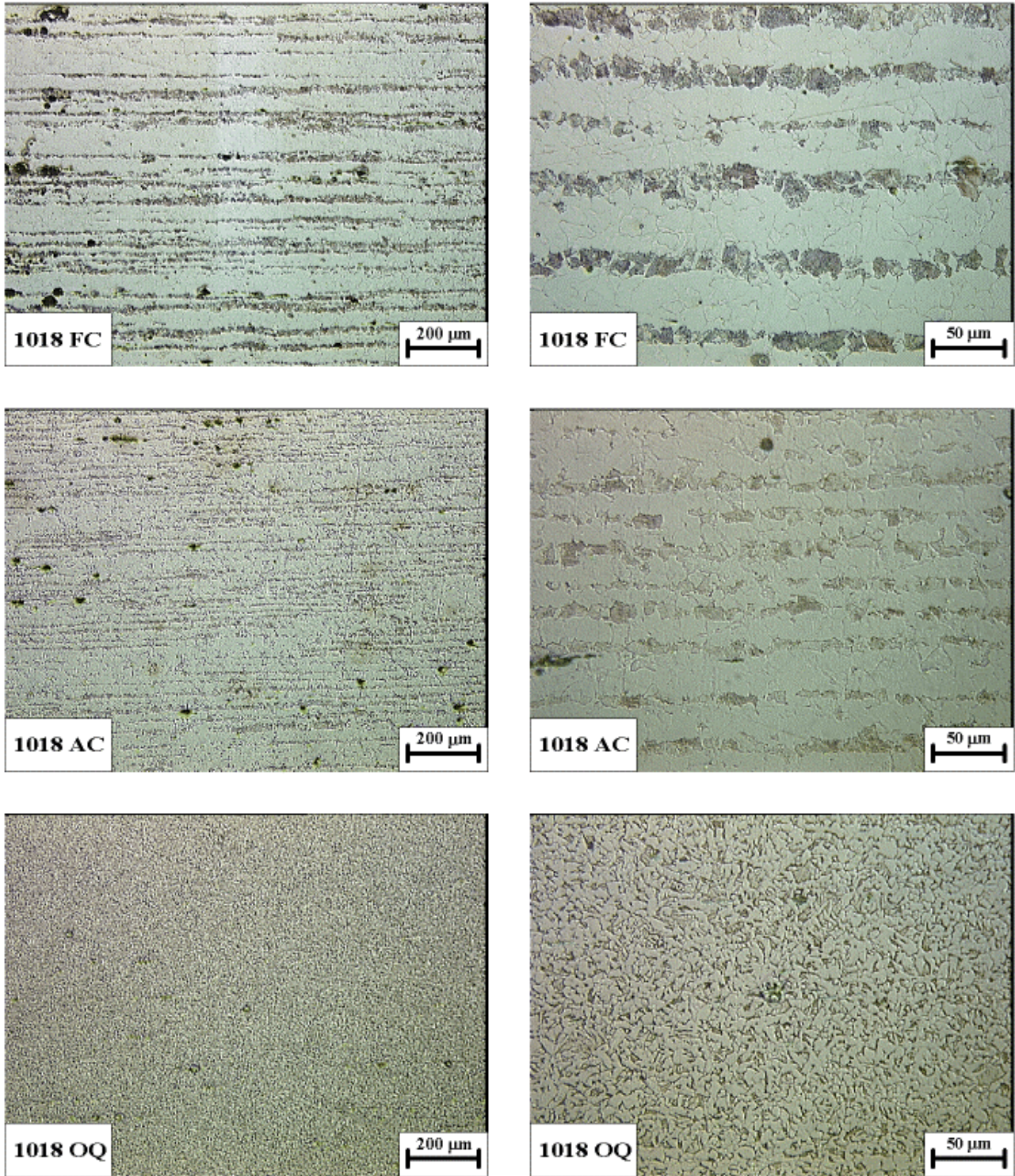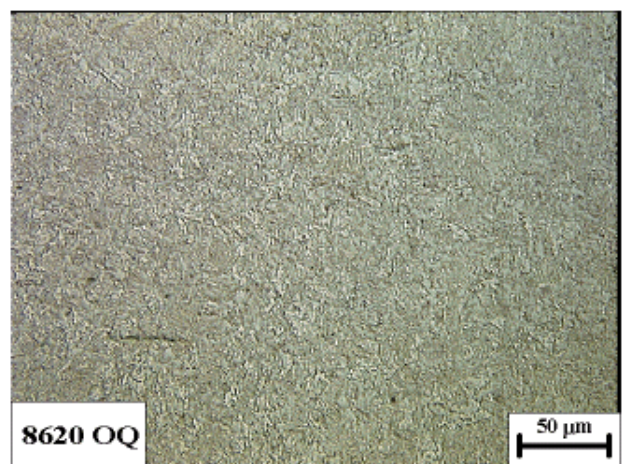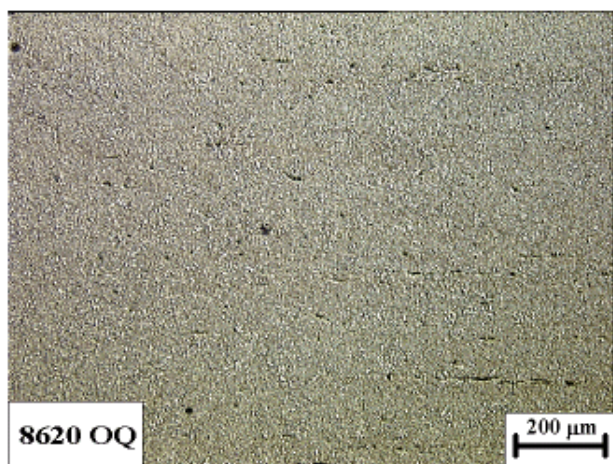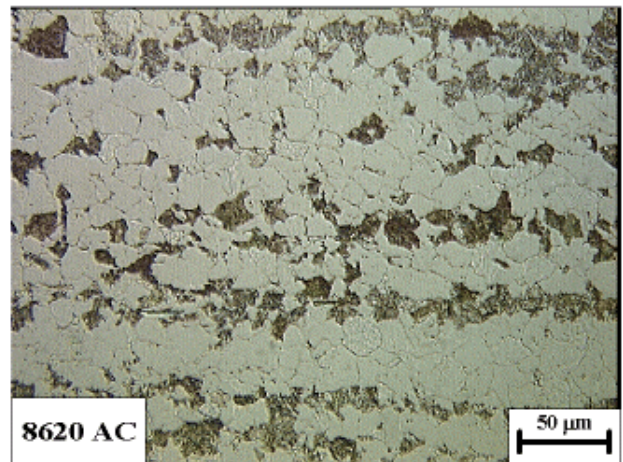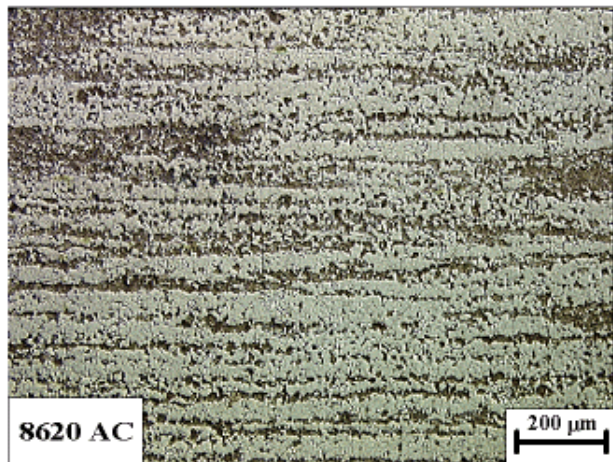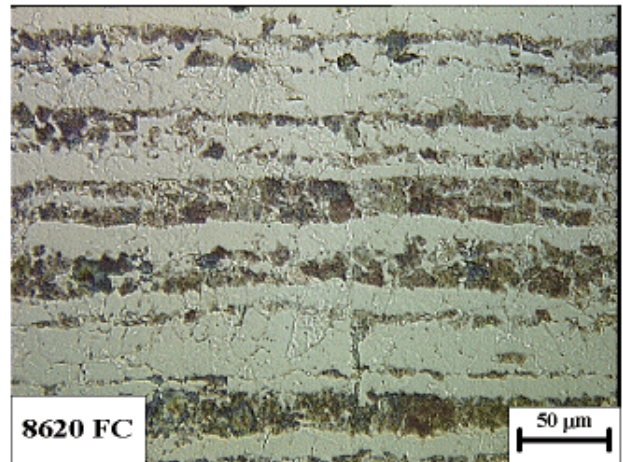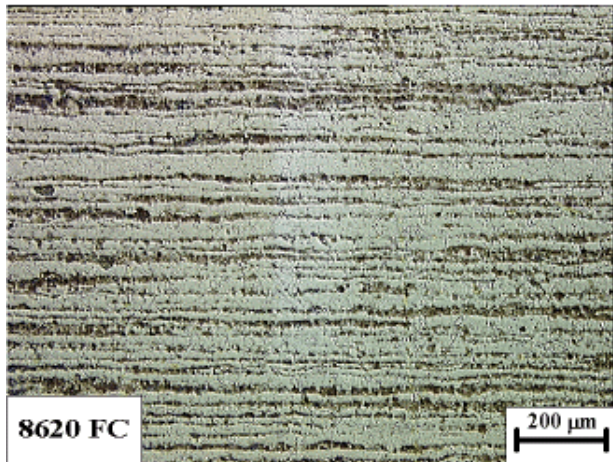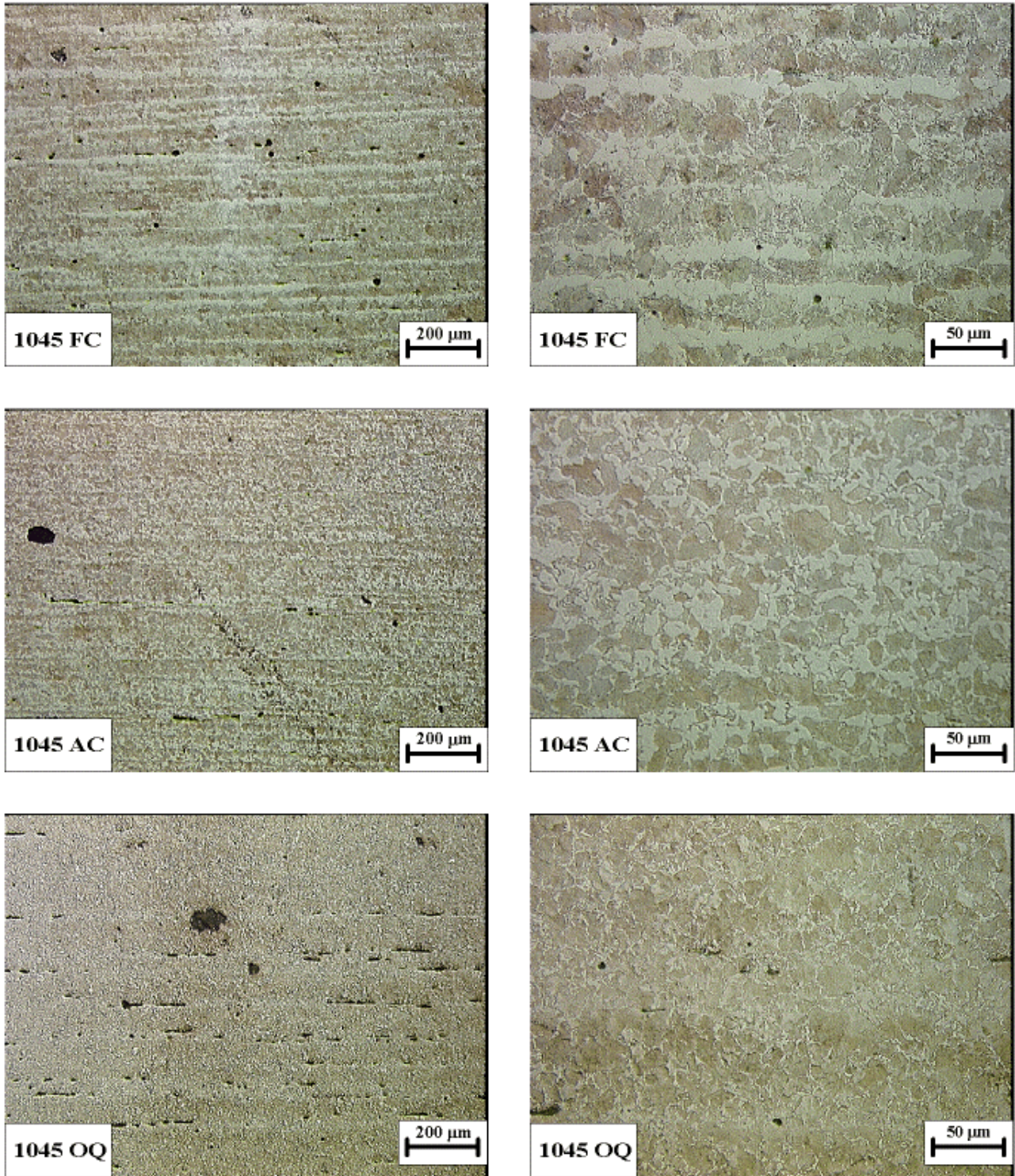Figure 4 – Microstructure of 1117 steel. Light optical micrographs, longitudinal sections, 2% nital etch.

1018

Figure 5 – Microstructure of 1018 steel. Light optical micrographs, longitudinal sections, 2% nital etch.

8620

Figure 6 – Microstructure of 8620 steel. Light optical micrographs, longitudinal sections, 2% nital etch.

1045

Figure 7 – Microstructure of 1045 steel. Light optical micrographs, longitudinal sections, 2% nital etch.
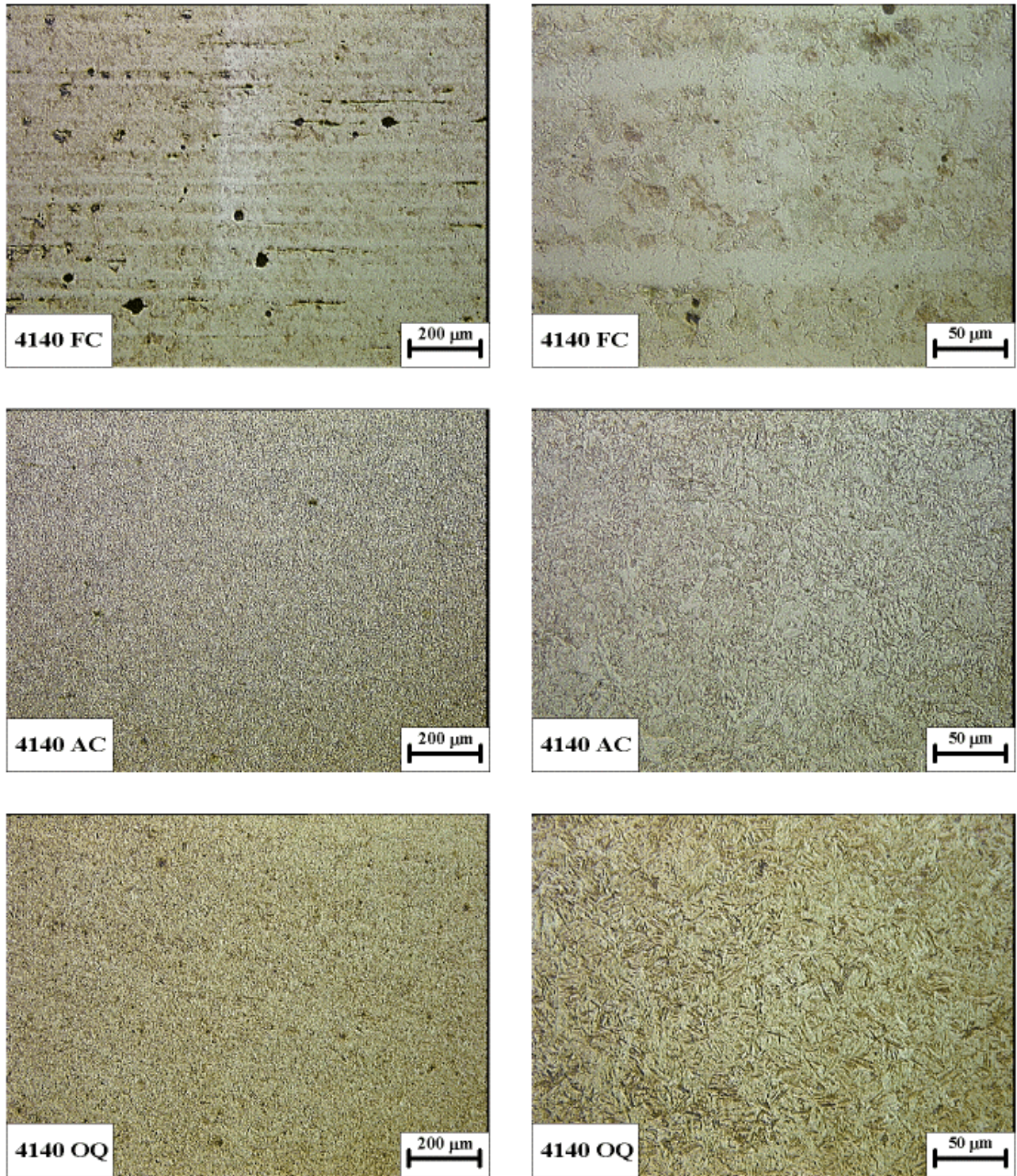
4140

Figure 8 – Microstructure of 4140 steel. Light optical micrographs, longitudinal sections, 2% nital etch.
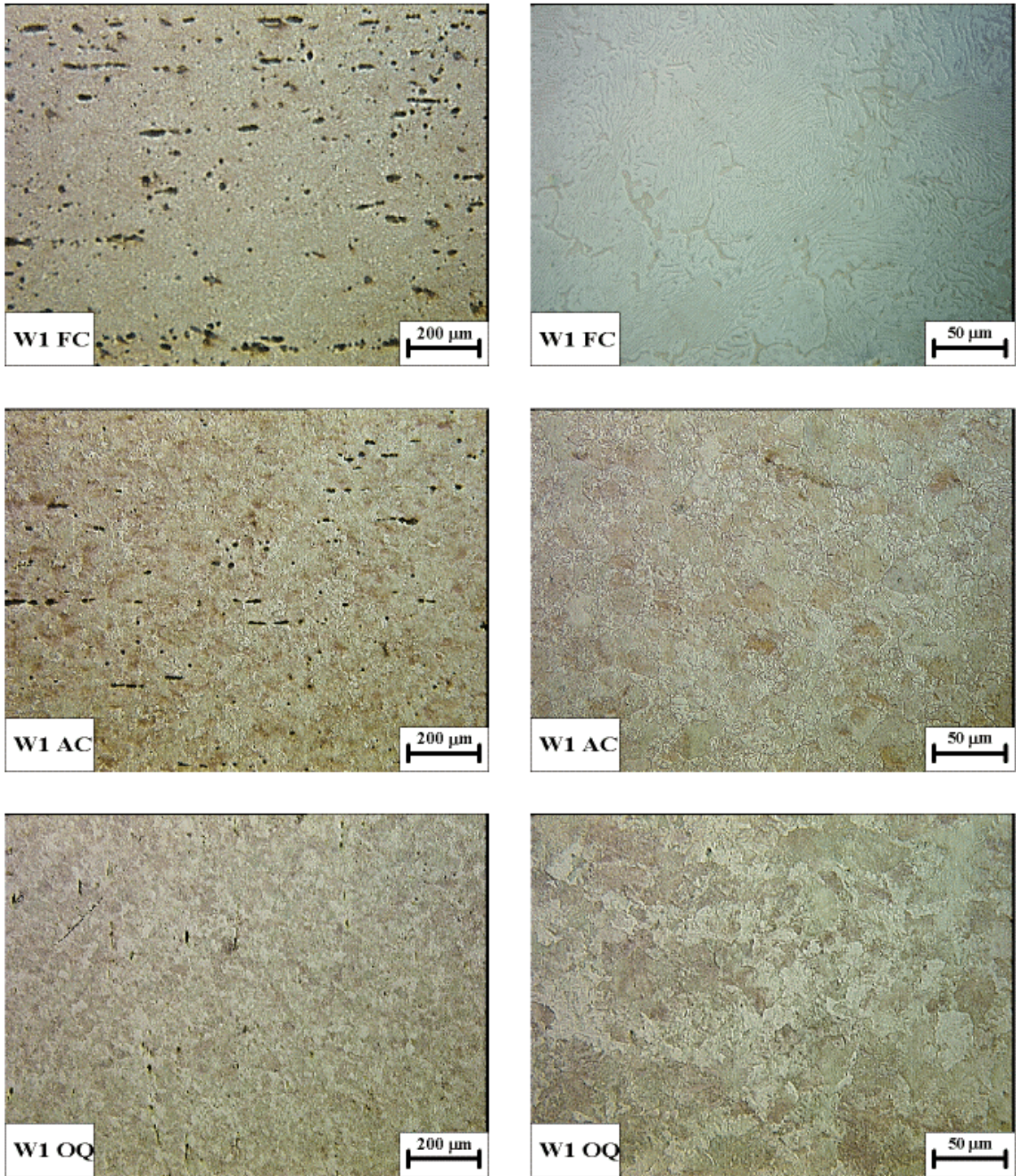
W1

Figure 9 – Microstructure of W1 steel. Light optical micrographs, longitudinal sections, 2% nital etch.
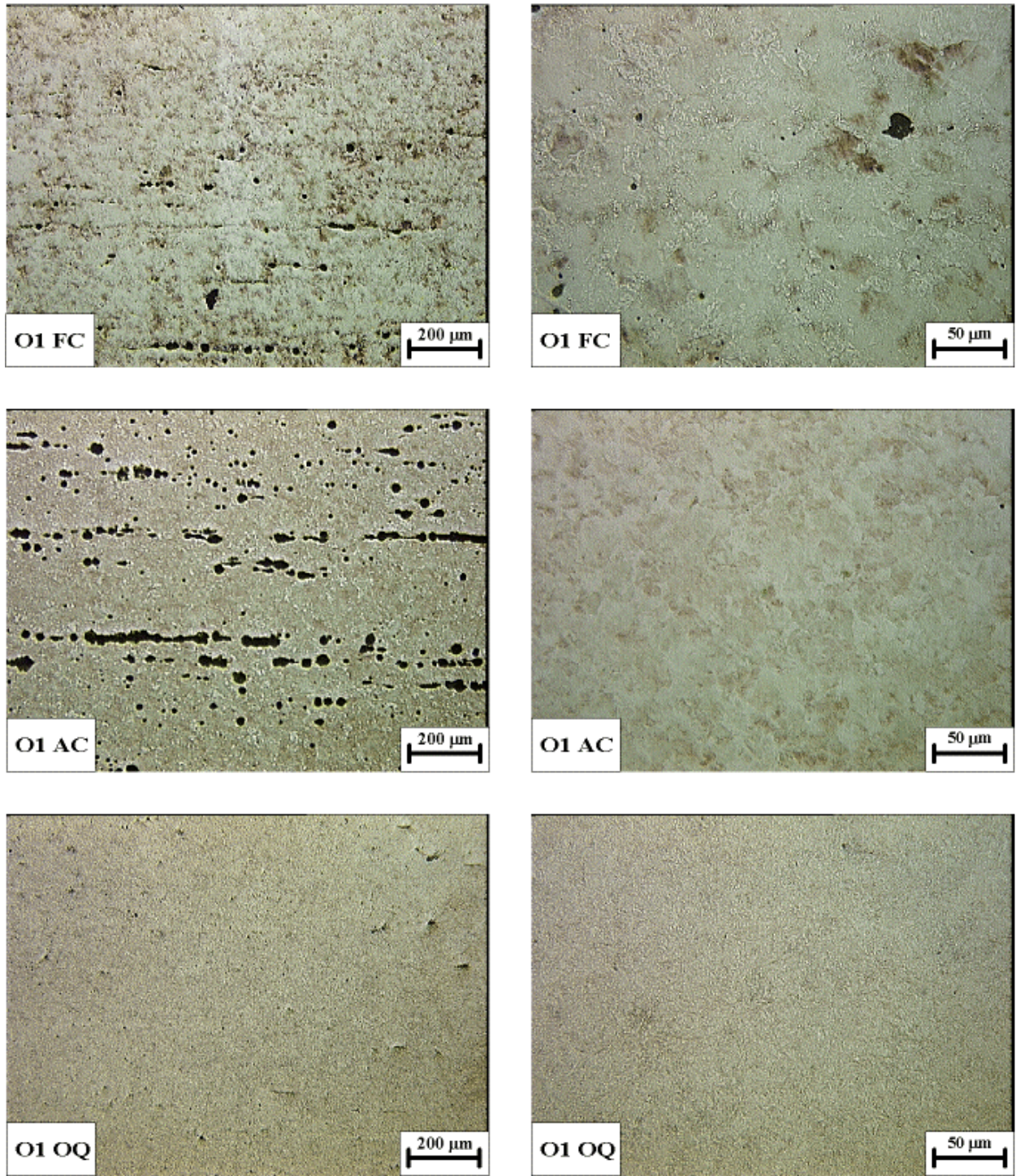
O1

Figure 10 – Microstructure of O1steel. Light optical micrographs, longitudinal sections, 2% nital etch.
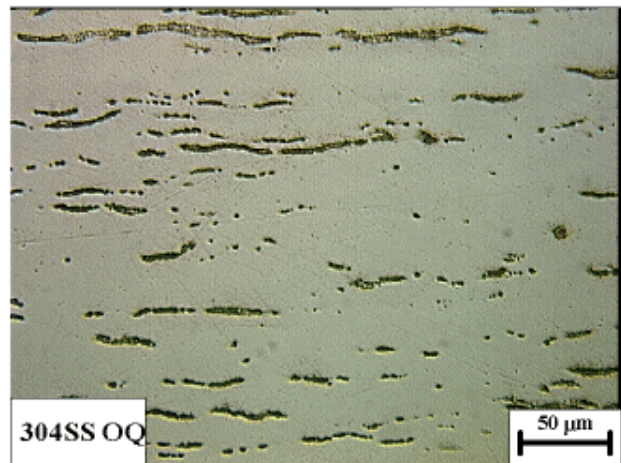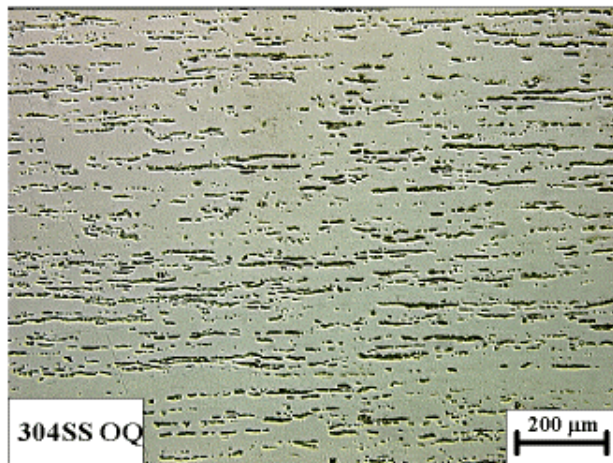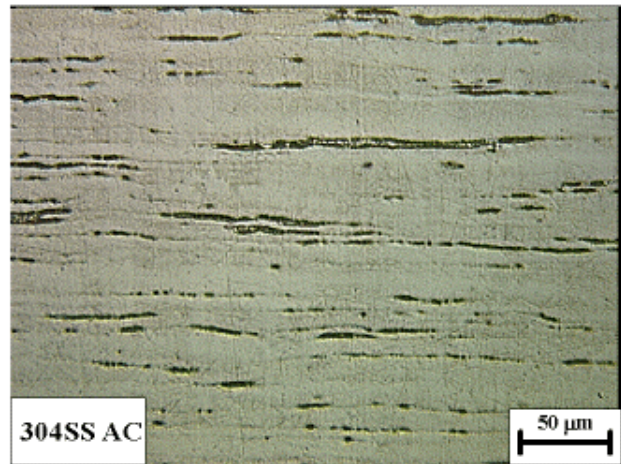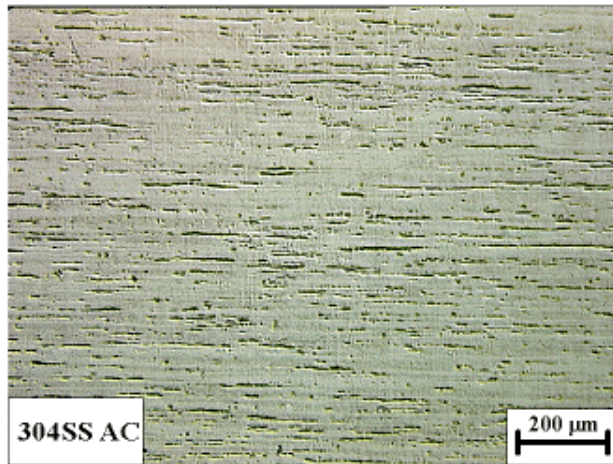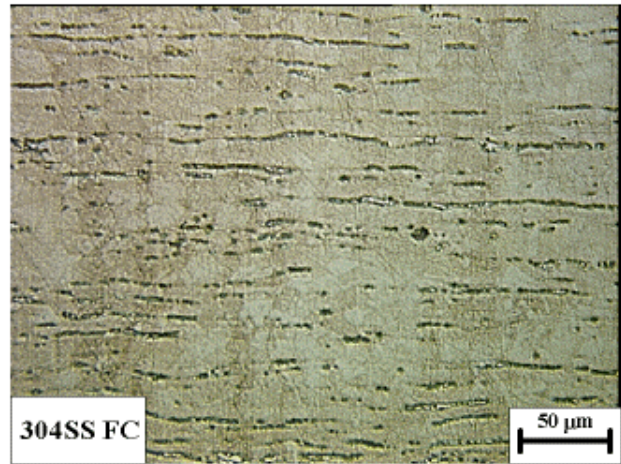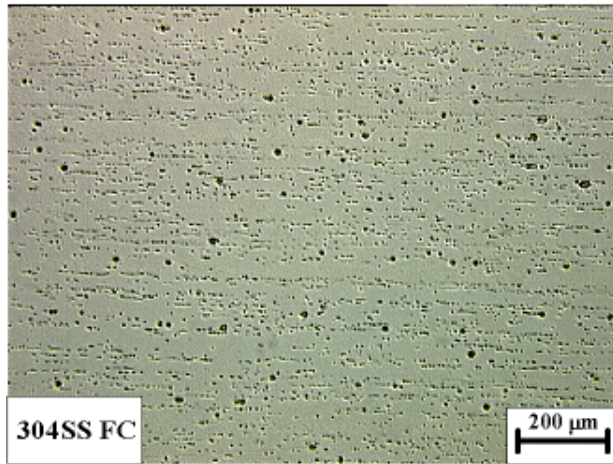
304SS

Figure 11 – Microstructure of 304SS. Light optical micrographs, longitudinal sections, Marbles etch.
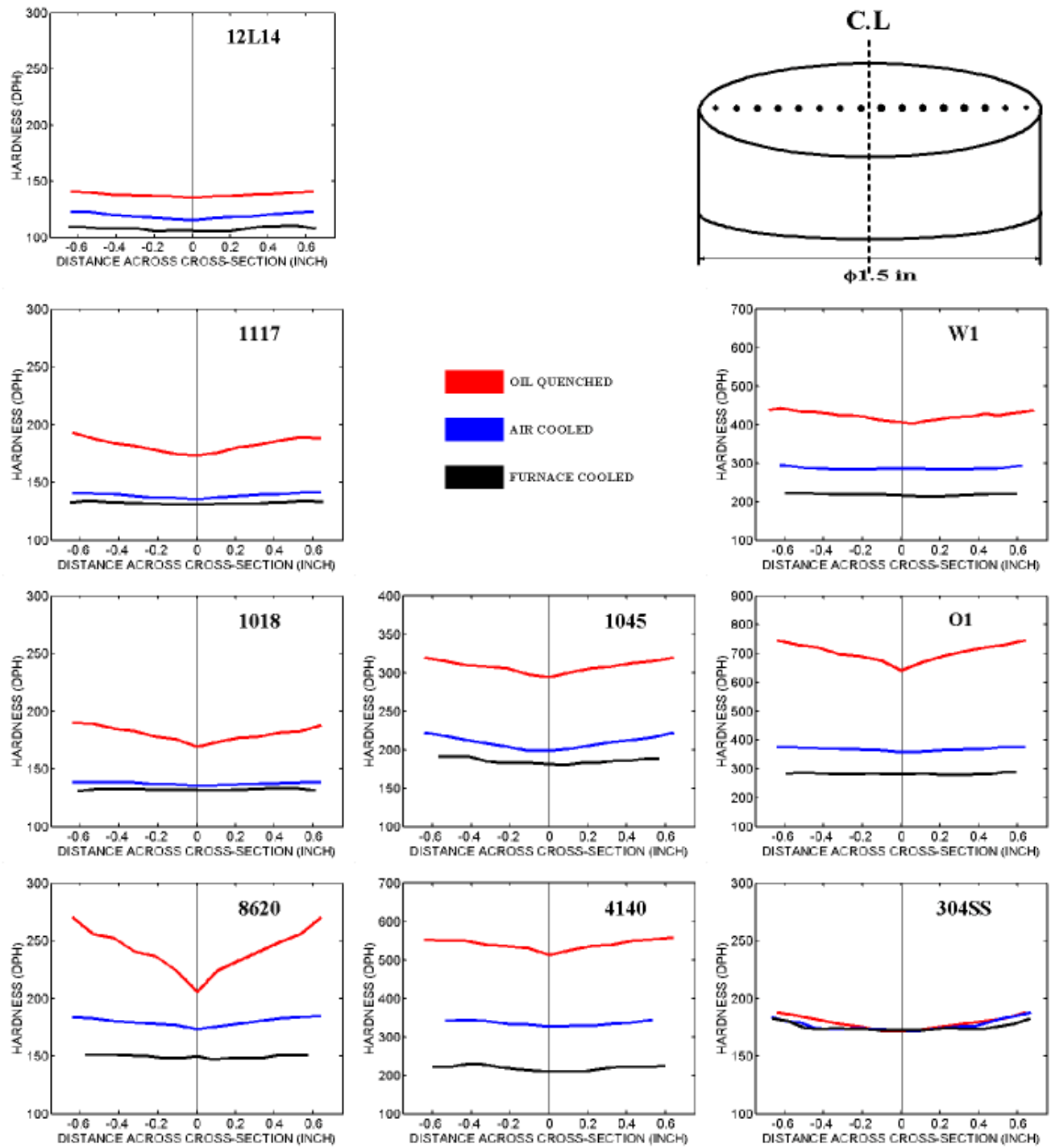
Figure 12 – Hardness profiles across the cross-sections of 1.5in dia bars used to machine the Jominy bars.

Hardness and Distortion profiles:

Figure 13 and 14 show the hardness and distortion pattern for the bars for the experimental conditions mentioned before, the following phenomenons are observed from the hardness and the distortion profiles of various steels used in analysis.

Low-Alloy Steels 12L14, 1117, 1018, 8620:

These steels exhibit Jominy hardness curves that start off above the valid HRB scale range at J1 and decrease rapidly with increasing distance from the quenched end and level off at hardness values between 70 and 85 HRB. The curves are generally consistent with published data. e.g. The Timken Company's Practical Data for Metallurgists.

The plots in the first column of Figure 13 shows that all the hardness curves follow a similar pattern and the effect of the prior microstructure has no effect on the hardenability.

The corresponding diameter distortion data illustrate that there is a characteristic expansion / contraction behavior that occurs with increasing distance from the quenched end that is similar for all low-carbon steels. In these steels, a maximum expansion is found at the quenched end that corresponds to 0.2pct or 0.002 in across the diameter.

The plots in the first column of Figure 14 shows that even though the shape of the distortion follows a similar trend the magnitude varies and the prior microstructure has little effect on the distortion profiles.

The position and magnitude of the minimum diameter change is not similar but has the largest negative value for the 1018 steel bars and the smallest negative value for the 8620 steel bars. At distance greater than approximately 1.5in (J24), the diameter of all bars increases to a level at or above the prequench sample diameter.

Low-Alloy Steels 1045 and 4140:

Higher end quench hardness is associated with higher carbon content as compared to the steels containing 0.2wt% carbon or less. Both 1045 and 4140 steels show similar hardness profile up to J10 position for all prior cooling rates. The order of magnitude of slight variation in hardness after the J10 position does not relate to the initial cooling rate.

The plots in the second column of the figure 13 shows that the prior microstructure has no effect on the hardness curves of 1045 and 4140.

Higher max distortion in J0 position is associated with a larger specific volume change due to dependence of martensite specific volume on carbon content [1]. Distortion profiles of the 1045 are somewhat magnified version of the 1018 distortion patterns indicating the effect of carbon content on the microstructure and distortion patterning is generally similar. The shape of the 4140 distortion curves is more abrupt as the depth to which the contraction extends is limited to
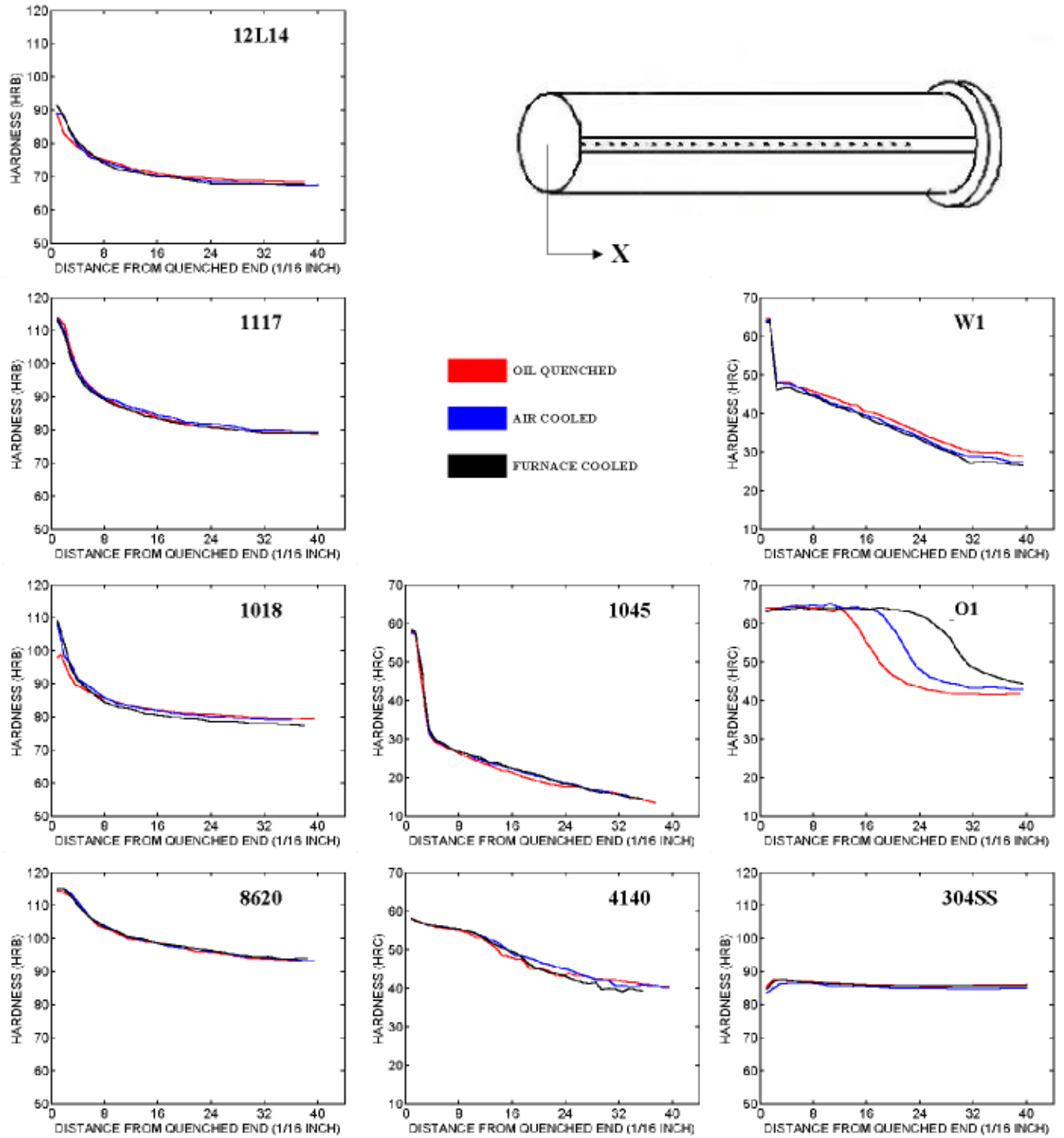
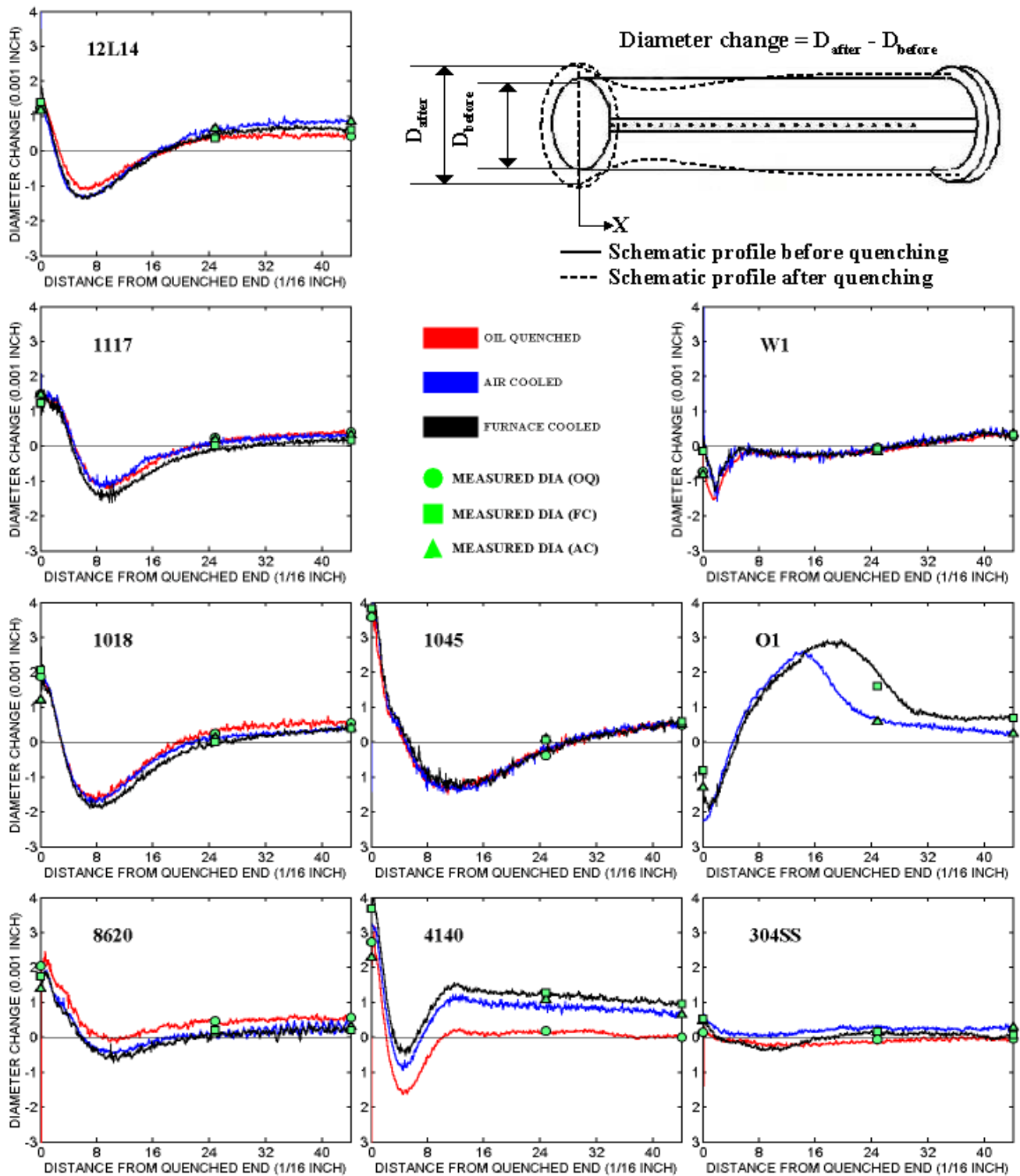Figure 13 – End quench bar hardness profiles of the steels used for the investigation.

Figure 14 – Distortion profiles of the steels used in the investigation.

less than 0.75 in (J12). The diameter change in the 4140 samples at distances greater than approximately 0.75 in show a dependence on pretreatment thermal treatment in which the diameter change is largest for the samples that was initially furnace cooled, then for the air-cooled sample and finally for the oil quenched pretreatment.

The plots in the column 2 of Figure 14 show that prior cooling rate has no apparent effect on the distortion profiles of the 1045 steel bars whereas in the case of the 4140 steel bars the results order with prior cooling rate and suggests the austenitizing treatment was unable to eliminate the effects of the prior treatments. Similar behavior was previously reported in 4340 samples by Kenyeri [3]. In that study, the difference was attributed to differences in alloy carbide dissolution kinetics and is also the likely cause of the behavior.

Tool Steel W1:

The plot in the column 3 of Figure 13 for W1 shows that prior heat treatment has no apparent effect on the hardenability and the plot in the column 3 of Figure 14 shows that the prior heat treatment has no effect on the distortion profiles either.

Variation in hardness is most rapid between J1 and J2 where the hardness decreases from approximately 65 to 48 HRc. The magnitude of the hardness curves decreases with decrease in rate of prior cooling approximately after the J3 position. In spite of the relatively high carbon content (1 wt-pct) and the high hardness at J1, the variation in diameter change is substantially less than is observed in all other steel, excepting the stainless steel. This rapid change in hardness and the small variation in distortion is likely a result of low hardenability of the steels and a transformation sequence, similar to that which occurs in carburized components, in which the diffusion-controlled transformation starts subsurface before the surface region reaches the martensite start temperature.

Tool Steel O1:

The plot in the column 3 of Figure 13 for O1 shows that prior heat treatment largely affects the hardness profile of the O1 steel bars and the plot in the column 3 of Figure 14 for O1 shows that the prior heat treatment has significant effect on the distortion profiles too.

The distortion results of the O1 steels are inverse to the behavior of the low-carbon steels. With increasing distance from the quenched end, the distortion pattern is one in which slight contraction is followed by a relatively large expansion before approaching zero. The volume contraction in the tip may be due to the retained austenite. High alloy content influences the deviant behavior of O1 steel bars. A similar behavior could be noticed in bars of other materials if reheated for a shorter time. Furthermore the O1 steel, similar to the 4140 steel, also exhibits a dependence on the prior thermal treatment in which separation is found to occur between the air-cooled and the furnace-cooled samples. The maximum distortion in the furnace-cooled sample is noticed at approximately 1.1in from the quenched end and this also coincides with the start of rapid decrease in the hardness in the hardness profile curves (J18). Similarly in the case of the O1 air-cooled sample the peak distortion and the start of rapid slide in the hardness value starts at J13. Since the O1 oil-quenched sample showed quench cracks the distortion could not be

measured but based on the correlation between the distortion and hardness results for the air-cooled and furnace-cooled sample it can be predicted that the peak distortion in O1 oil-quenched sample will be at approximately J8 position where the rapid slide in hardness value starts in the hardness profile. The distortion results of O1 oil-quenched bar could not be obtained due to difficulty in carrying out the process.

Stainless Steel 304:

The 304SS Jominy data indicate that slight, although measurable, variations in hardness and dimensional change occur with increasing distance from the quenched end. This result, together with those from the other steels, illustrate unambiguously that the majority of the hardness and dimensional changes observed in end-quench tests are attributable to the influence of cooling rate on the microstructure of austenite decomposition.

The slight increase and then decrease in hardness with distance from the quenched end in the SS samples may be attributed to the Cr-carbide precipitation reaction in carbon-containing stainless steels and the variation in the size distribution of such carbides ($Cr_{23}C_6$) that is typically expected in quench-aging or precipitation hardening microstructures [6].

SUMMARY

Collectively the results show the prior microstructure has very little effect on Jominy hardenability curve for all steel bars except the O1 bars and this hardenability result is in confirmation with the already published data [7]. A shorter reheat time could have given a spread of distortion profile pattern in case of other steel bars. For the reheat time employed the effect of prior microstructure in distortion is noticeable only in the case of O1 and 4140 steel bars.

For the experimental conditions used, the results can be summarized as follows:

1) The ferrite grain size refines and the microstructural banding gets denser as the cooling rate is increased while producing various starting microstructure.

2) The hardness profile across the 1.5in bars uniformly show hardness decrease towards the center due to the decrease in the cooling rate towards the center.

3) All steels show a Jominy hardness profile that decrease with the J position; the rate of decrease is determined by the hardenability of the steels.

4) The wide difference in the hardness profile is noticed in the case of the O1 tool steel.

5) The distortion profiles of the Jominy bars of all steels except that of the O1 tool steel is such that the maximum growth in diameter occurs at the tip and in the case of O1 tool steel the maximum shrinkage occurs at the tip.

6) This magnitude of the maximum growth varies with the chemical composition and the initial microstructure.

7) The maximum shrinkage for all materials except O1 tool steel occurs between J2 to J12 positions and in case of O1 tool steels the maximum growth is noticed at J positions below the tip.

8) The magnitude of the maximum shrinkage and the J position at which it occurs varies with the composition of the steels and the initial microstructure.

9) In general the distortion profile follows an hourglass shape though with varying magnitude in case of all steels except the O1 tool steel, in which case it shows a mirror image of the distortion profile noticed in other steels.

REFERENCES

1. *Cook, W.T.,* "Review of Selected Steel-related Factors Controlling Distortion in Heat-treatable Steels," Heat Treatment of Metals, v 26 n 2, 1999, pp 27-36.

2. *Fukuzumi, T., Yoshimura, T.*; "Reduction of distortion caused by heat treatment on automobile gear steels," Proceedings of the first international conference on quenching and control of distortion, Chicago, Illinois, USA, 22-25 September 1992, pp 199-203.

3. *Kenyeri, R., and Foley, R.P.,* "Effects of Prior Microstructure on Hardness and Shape Variability in 1018 and 4340 Steel Jominy Bars," Proceeding of the Jerome B. Cohen Symposium on Residual Stresses, held 11-14 October 2000 in St. Louis, MO, ASM International, Materials Park, OH, 2001 (in press).

4. *Berns, H.*, "Distortion and Crack Formation by Heat Treatment of Tools," Radex Rundschau, v 5 n 1, April, 1989, pp 40-57.

5. Standard Method of End-Quench Test for Hardenability of Steel, *ASTM* standard 255, ASTM Headquarters, 1916 Race St, Philadelphia, PA 19103.

6. *Leslie, W.C.,* "The Physical Metallurgy of Steels," Tech Books, 2600 Seskey Glen Court, Herndon, VA 22071.

7. *Roberts, G., Krauss, G., Kennedy, R.;* "Tool Steels fifth ed.," ASM International, Material Park, Oh 44073-0002.

ACKNOWLEDGEMENT